ELSEVIER

Spectrochimica Acta Part B 60 (2005) 479–490

SPECTROCHIMICA ACTA PART B

www.elsevier.com/locate/sab

Laser-induced breakdown spectroscopy for space exploration applications: Influence of the ambient pressure on the calibration curves prepared from soil and clay samples

Béatrice Sallé[a,*], David A. Cremers[b], Sylvestre Maurice[c], Roger C. Wiens[d]

[a]CNRS, INSU, 3 rue Michel Ange, BP 287, 75766 Paris Cedex 16, France
[b]Los Alamos National Laboratory, Advanced Chemical Diagnostics and Instrumentation Group, MS J565, Los Alamos, NM 87545, USA
[c]Observatoire Midi-Pyrénées, Centre d'Etude Spatiale des Rayonnements, 9 avenue du Colonel Roche, 31400 Toulouse, France
[d]Los Alamos National Laboratory, Space and Atmospheric Sciences Group, MS D466, Los Alamos, NM 87545, USA

Received 4 October 2004; accepted 16 February 2005
Available online 31 March 2005

Abstract

Recently, there has been an increasing interest in the laser-induced breakdown spectroscopy (LIBS) technique for stand-off detection of geological samples for use on landers and rovers to Mars, and for other space applications. For space missions, LIBS analysis capabilities must be investigated and instrumental development is required to take into account constraints such as size, weight, power and the effect of environmental atmosphere (pressure and ambient gas) on flight instrument performance. In this paper, we study the in-situ LIBS method at reduced pressure (7 Torr CO_2 to simulate the Martian atmosphere) and near vacuum (50 mTorr in air to begin to simulate the Moon or asteroids' pressure) as well as at atmospheric pressure in air (for Earth conditions and comparison). Here in-situ corresponds to distances on the order of 150 mm in contrast to stand-off analysis at distance of many meters. We show the influence of the ambient pressure on the calibration curves prepared from certified soil and clay pellets. In order to detect simultaneously all the elements commonly observed in terrestrial soils, we used an Echelle spectrograph. The results are discussed in terms of calibration curves, measurement precision, plasma light collection system efficiency and matrix effects.

Keywords: Laser-induced breakdown spectroscopy; Reduced pressure; Matrix effects; Soils; Clays; Space applications

1. Introduction

The laser-induced breakdown spectroscopy (LIBS) technique has been proposed as a new method that could be installed on landers and rovers for stand-off detection of geological samples on planetary surfaces [1–6]. LIBS is based on the focusing of a high-power pulsed laser beam (≥ 1 GW/cm^2) onto a sample surface leading to the creation of a plasma composed of excited species which emit light. Collection of the plasma light, followed by spectral dispersion and detection, permits identification of the elements present in the sample using their characteristic spectral lines and allows quantitative analysis. This technique has been applied to many samples such as solids in hostile environments [7], liquids [8,9], gases [10] and, environmental and geological samples [11–14]. For space exploration, this method possesses several advantages compared to other techniques which have been used on past and current missions (examples at Mars: X-Ray Fluorescence on the Viking 1 and 2 missions [15,16], Alpha-Proton-X-Spectroscopy on the Pathfinder mission [17] and the Mars Exploration Rover missions in progress). These advantages include: stand-off analysis capability [5,18,19], no sample preparation required, rapid analysis (few minutes), simultaneous multi-elemental detection (major, minor and trace elements), and

* Corresponding author. CEA Saclay, DEN/DPC/SCP/LRSI Bât. 391 91191 Gif sur Yvette Cedex, France. Tel.: +33 1 69 08 77 37; fax: +33 1 69 08 77 38.
E-mail address: salle@carnac.cea.fr (B. Sallé).

0584-8547/$ - see front matter © 2005 Elsevier B.V. All rights reserved.
doi:10.1016/j.sab.2005.02.009

the ability to measure the composition of weathered layers and the underlying bulk rock composition through depth profiling (repeated ablation). For space applications, LIBS analysis capabilities must be investigated and instrumental development is required to take into account constraints such as size, weight, power and environmental atmosphere (pressure and ambient gas) imposed on flight instruments. Because of the different environmental atmospheres to be found on Mars, the Moon, and asteroids, studies are needed to understand analytical requirements and performance under such conditions. In this paper, we characterize the in-situ LIBS method at reduced pressure (7 Torr CO_2 for Mars) and near vacuum (50 mTorr in air to begin to simulate the Moon and asteroids) as well as at atmospheric pressure in air (585 Torr for Los Alamos atmospheric conditions and comparison). Here in-situ corresponds to a close distance of several centimeters in contrast to stand-off analysis at many meters distance. This characterization is important because the excitation properties of the LIBS plasma are strongly dependent on the pressure of the surrounding atmosphere, which can have a strong effect on the detection of elements in a solid [3–5,20–29]. We studied the influence of the ambient pressure on calibration curves prepared using certified soil and clay pellets containing elements commonly observed in terrestrial soils (e.g. Al, Ba, Ca, Cr, Fe, K, Li, Mg, Mn, Na, Ni, Si, Sr, Ti). Results are presented for in-situ analysis including measurement precision for quantitative analysis and the pressure dependence of matrix effects. We also studied the possibility of using non time-resolved spectra acquisition at low pressures and the influence of the plasma light collection system on the analytical results obtained at reduced pressures.

2. Experimental setup

For testing in-situ analysis by LIBS at different pressures, we used the experimental setup presented in Fig. 1. Special care was taken to reproduce some important experimental conditions expected in space exploration, especially for the laser in terms of wavelength, pulse repetition rate and energy. Q-switched Nd:YAG laser pulses (Spectra Physics INDI operating at 1064 nm and 10 Hz) were focused with a 150 mm focal length lens (25 mm diameter) onto the sample surface. The laser energy used for plasma formation was 40 mJ (laser irradiance = 28 GW/cm^2) which is considered to be in the energy range achievable by a compact laser likely to be incorporated on landers or rovers. The samples were placed in a chamber in which the pressure could be adjusted between atmospheric pressure and 50 mTorr. The chamber could also be filled with a flowing CO_2 gas in order to simulate the Martian atmosphere. Light from the plasma was collected at a small angle to the axis of the incident laser pulses in one of two ways. The light was either focused with a 100 mm focal length lens (50 mm diameter) onto a fused silica optical fibre (length = 1 m, core diameter = 1 mm) or the fibre was pointed at the plasma and light collected without a lens. The end of this fibre was directly connected to the entrance slit of an Echelle spectrograph (ESA 3000, LLA) equipped with an Intensified Charge-Coupled Device (ICCD) camera detector system (KAF 1000, Kodak). The advantage of this device is its ability to simultaneously collect the entire 200–780 nm spectral range with a resolving power $\lambda/\Delta\lambda \sim 10{,}000$. Since chromatic aberrations existed in this setup due to the light collection lens, the entire spectral range of 200–780 nm could not be observed simultaneously with strong intensity. The focus of the plasma light on the optical fibre was adjusted to give maximum intensity in the 400–600 nm spectral region.

For space applications, compact integrated spectrograph and detection systems are available commercially but because of their small size and mass, these devices have no intensified detectors, and the associated temporal gating of the emission signal can not be used in the usual way [30]. An evaluation of these commercial compact systems is in

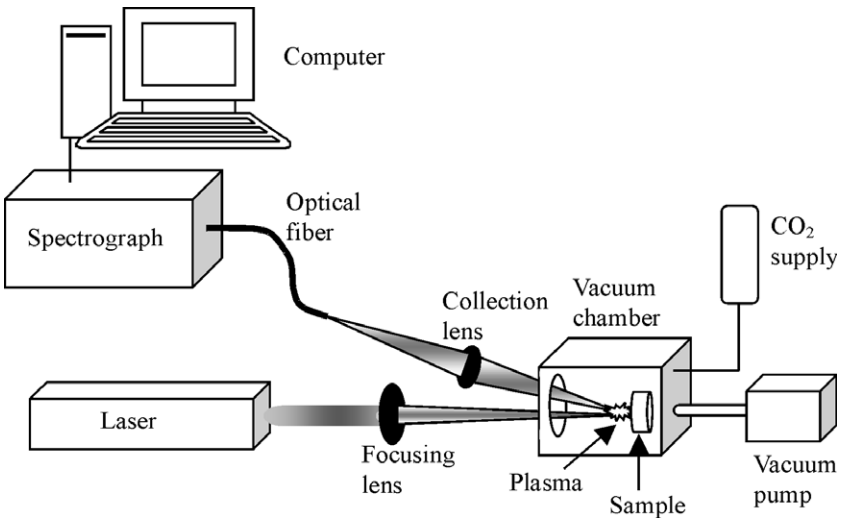

Fig. 1. Experimental setup used for LIBS at different pressures.

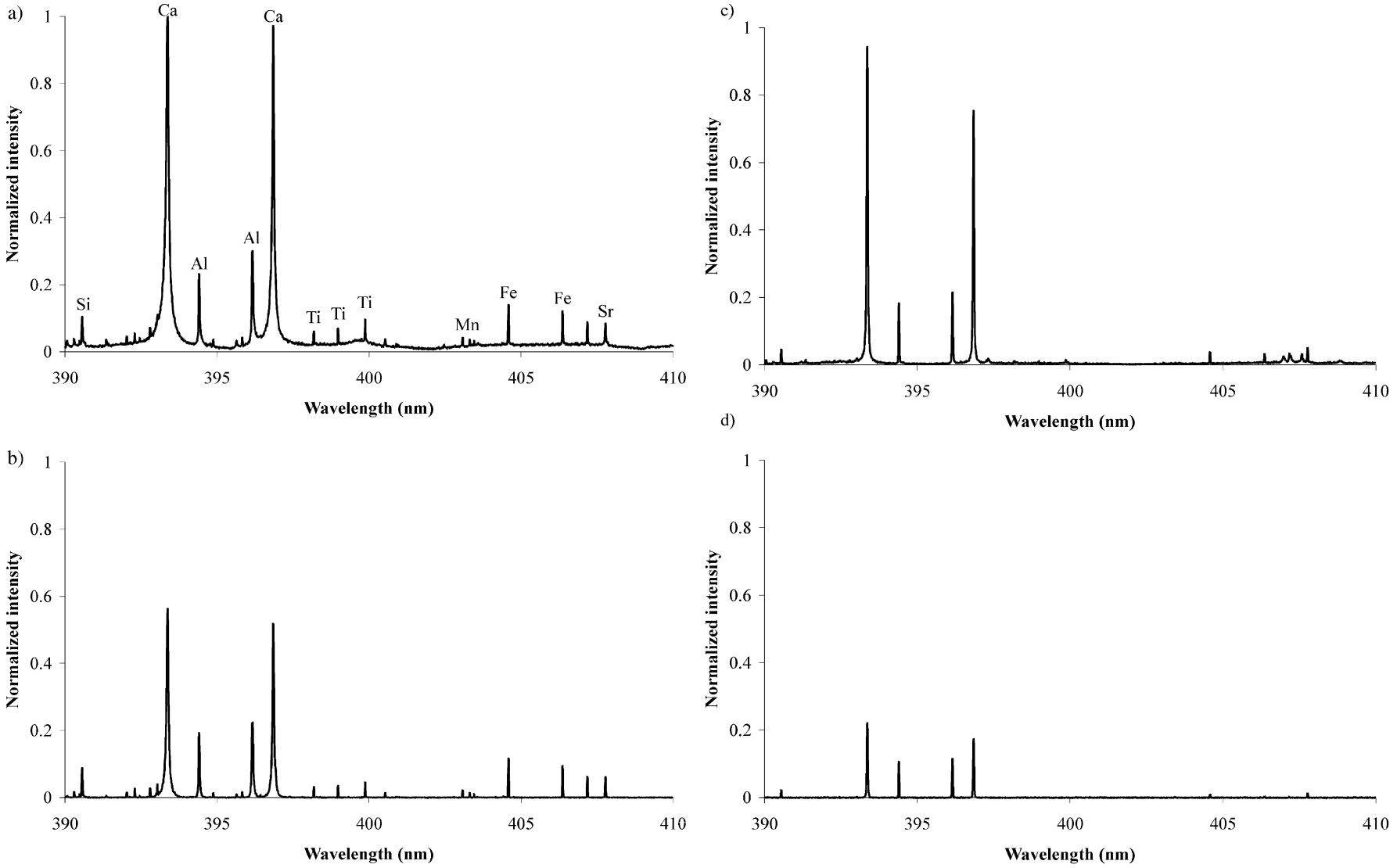

Fig. 2. LIBS spectra obtained from one soil (sample GBW 07301) at 400 nm: a) in air without temporal resolution; b) in air with a time delay of 1 μs; c) at 7 Torr of CO_2 without temporal resolution; d) at 7 Torr of CO_2 with a time delay of 1 μs.

Table 1
Signal to background ratio for different lines obtained at atmospheric pressure in air and 7 Torr of CO_2, without temporal resolution and with a time delay of 1 μs

Element (line)	585 Torr in air		7 Torr of CO_2	
	Delay 0	Delay 1 μs	Delay 0	Delay 1 μs
Al (396.15 nm)	6.7	29.1	24.8	214
Ca (393.37 nm)	12.1	36.5	48.6	329.7
Fe (404.59 nm)	4.3	321.1	7.8	180.5
Mn (403.31 nm)	1.6	59.4	1.7	Undetected
Si (390.56 nm)	3.5	19.6	9	754
Sr (407.77 nm)	2.6	28.4	5	22.2
Ti (398.97 nm)	2.8	53.5	2.7	Undetected

progress in the laboratory [31]. To replicate the performance capabilities of these compact systems, we used the ESA 3000 Echelle spectrograph without temporal resolution (no time delay) and with a wide time gating (1 ms) in order to record the plasma emission over its entire lifetime. Results obtained in such conditions were compared with those recorded with a time delay between ICCD camera gating and the laser pulse. The time resolution was controlled by a programmable pulse delay generator (DG 535, Stanford Research Systems). The plasma light was integrated over 50 laser shots, a reasonable number for a compact laser likely to be incorporated on a rover. The intensifier gain (G) was maintained to a constant value in all experiments (typically G=1800, with a maximum of G=4000 possible). Because the commercial compact spectrograph/detector system under investigation for space applications has no intensifier, we verified that G=1800 on the ESA 3000 spectrograph corresponded closely to a non-intensified system. This was realized by recording with the ESA 3000 spectrograph and one version of the compact spectrograph/detector system (HR2000, Ocean Optics, USA) the known spectral response of a continuous standard lamp. It was found that the standard lamp produced a signal of 270 photons (at 400 nm) using the Echelle spectrometer with G=1800 whereas a signal of 420 photons was produced by the HR2000 system, therefore yielding very similar intensity responses to 400 nm light.

Calibration curves were prepared for elements including Al, Ba, Ca, Fe, Mg, Mn, Na, Pb, Si, Sr and Ti using a series of certified standard samples obtained from the Brammer Standard USA: soils (GBW 07301, GBW 07304 to GBW 07312, GBW 07404) and clays (GBW 03101a, GBW 03102, GBW 03102a, GBW 03103, GBW 03115, IPT 28). The powder samples were transferred into an aluminum dish (32 mm diameter) and were compacted into a pellet using a force of approximately 20 t. These standard samples were chosen to simulate the composition of Martian soils but do not necessarily reproduce other characteristics (nevertheless the grain size of our samples was in the range of dust particle sizes expected on Mars [32,33]). Each point displayed on calibration graphs is a mean value calculated from 6 spectra (each spectrum is the average of 50 shots). The error bars were obtained with a confidence of 95%, inducing a Student t factor equal to 2.571. They were calculated from the formula $\frac{t\times\sigma}{\sqrt{n}}$ with n the number of replicates and σ the standard deviation.

3. Results and discussion

3.1. Effect of time resolution and pressure on spectra

A number of LIBS studies have used time resolution of the emission signal to enhance signal to background ratios by recognizing that different decay rates characterize the continuum and atomic emission processes [34]. Spectral interference may also be minimized by taking into account the differing relaxation times between different elements [35] and ionization stages. For LIBS analysis applied to space exploration, we are considering a very compact grating type spectrograph integrated in a single package with a CCD detector [30] as described above. This detector is not gated as are the more sophisticated gated-intensifier CCD arrays often used for LIBS. Signal acquisition without temporal resolution is planned for a LIBS flight instrument under development. Thus, we wanted to determine if analytically useful spectra could be obtained at reduced pressures without gating the detection system. We compare in Fig. 2, spectra obtained from one soil (sample GBW 07301) without temporal resolution (no gate pulse delay) to spectra obtained at a delay of 1 μs between the ICCD camera gate pulse and the laser pulse, at atmospheric pressure in air and at 7 Torr of CO_2. The gate width is 1 ms in both cases. In this figure, the spectra were normalized to the maximum intensity of the spectrum acquired without time resolution at atmospheric pressure in air. The time delay of 1 μs was chosen because it gave the highest signal to background ratio for the majority of studied elements at atmospheric pressure in air and 7 Torr of CO_2. At atmospheric pressure in air, a background continuum is emitted at the beginning of the plasma (Fig. 2a) evident as relatively featureless emission signals present at wavelengths not corresponding to element lines. Table 1 presents the signal to background ratio obtained for

Table 2
Full width at half maximum (FWHM in nm) of different lines obtained at atmospheric pressure in air and 7 Torr of CO_2, without temporal resolution and with a time delay of 1 μs

Element (line)	585 Torr in air		7 Torr of CO_2	
	Delay 0	Delay 1 μs	Delay 0	Delay 1 μs
Al (396.15 nm)	0.054	0.054	0.032	0.032
Ca (393.37 nm)	0.09	0.07	0.05	0.04
Fe (404.59 nm)	0.032	0.032	0.032	0.032
Mn (403.31 nm)	0.033	0.033	0.032	Undetected
Si (390.56 nm)	0.032	0.032	0.031	0.031
Sr (407.77 nm)	0.031	0.031	0.031	0.031
Ti (398.97 nm)	0.031	0.031	0.031	Undetected

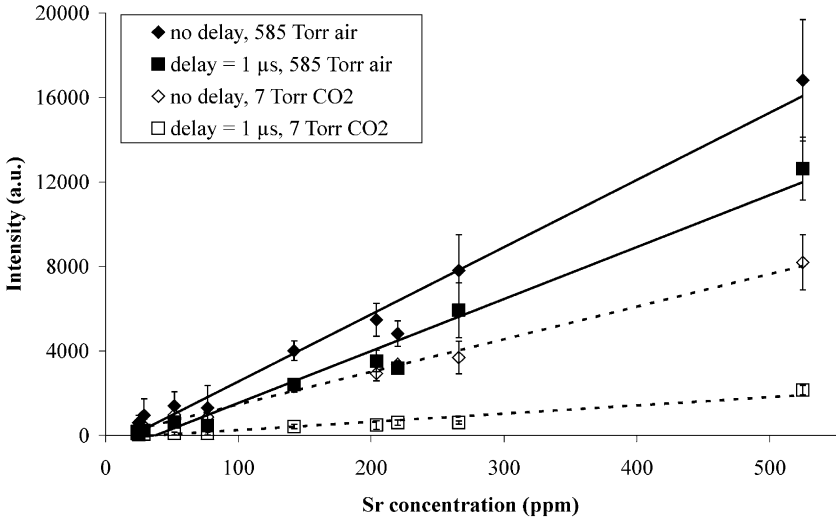

Fig. 3. Calibration curves of Sr (407.7 nm) prepared from soils without and with temporal resolution at atmospheric pressure in air and at 7 Torr of CO_2.

different lines at atmospheric pressure in air and 7 Torr of CO_2 without temporal resolution and with a time delay of 1 µs. The background was determined as the mean value of the off-line emission intensity measured at each side of the maximum intensity of the listed line. Without temporal resolution, the signal to background ratio is greater at 7 Torr of CO_2 than at atmospheric pressure in air. The use of time delay allows an increase in the signal to background ratio at both pressures. Table 2 gives the Full Width at Half Maximum (FWHM) of lines calculated for atmospheric pressure in air and 7 Torr of CO_2, without temporal resolution and with a time delay of 1 µs. Al and Ca lines show broadening at atmospheric pressure with no time resolution. With time resolution, the width of these lines decreases. At 7 Torr of CO_2, the line widths are lower than at atmospheric pressure in air. At 7 Torr of CO_2 and with time resolution, the emission signal becomes very low and not all the lines are detected. The FWHM of detectable lines from Fe, Mn, Si, Sr, Ti, shows little change with time resolution and pressure. These results are consistent with those obtained in Ref. [4] at high pressure: the elements that are present at concentrations of more than a few percent by weight in the sample (e.g. Al and Ca) and that have transitions originating from lower energy upper levels (<3.15 eV) that end at or near the ground state energy level (<0.02 eV) are those that show strong effects of a pressure increase by broadening/self-absorption. The observed Mn, Sr and Ti lines also have upper energy levels <3.13 eV that all end in the ground state but these show no significant broadening/self-absorption with pressure increase and these elements are present in the sample at concentrations lower than 1%. Elements that are present at concentrations higher than a few percent which do not exhibit the strong effects of pressure increase (e.g. Fe and Si) all have upper energy levels which are relatively high (>4.55 eV) and the transitions end in upper energy levels (>1.48 eV). The

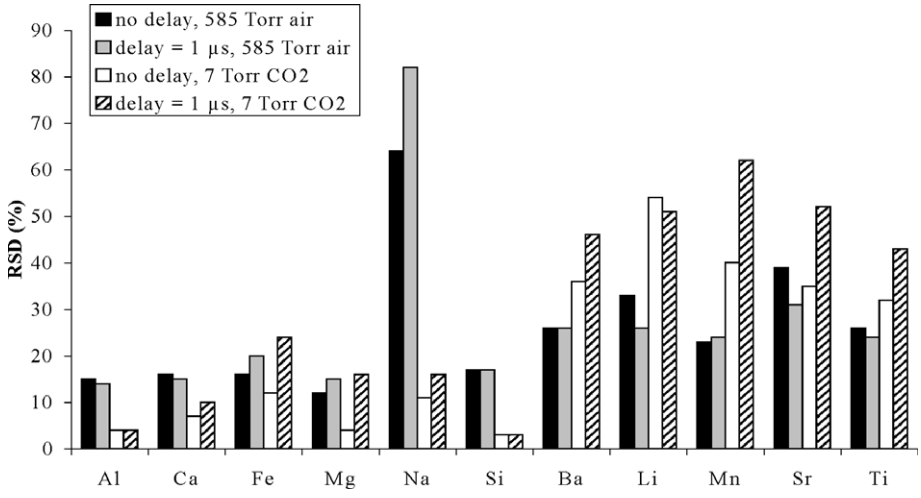

Fig. 4. Relative Standard Deviation (RSD) obtained from calibration curves in soils without and with temporal resolution at atmospheric pressure in air and at 7 Torr of CO_2.

concentration of elements and the energy levels of the transition appear to be the main factors affecting broadening and self-absorption.

These results show that analytically useful spectra can be obtained without gating the detection system, especially at reduced pressures where broadening and self-absorption are less important and the background continuum is reduced compared to atmospheric pressure.

3.2. Effect of time resolution on calibration curves

Fig. 3 depicts calibration curves of Sr (407.7 nm) prepared from soils without temporal resolution and with a time delay of 1 μs at atmospheric pressure in air and at 7 Torr of CO_2. For the two pressure conditions, the slope of the calibration curves (which represents the sensitivity) without time resolution is greater than the slope with time delay. The use of a higher gain of the ICCD with a 1 μs time delay would lead to more sensitive detection, i.e. a calibration curve with greater slope. But to reproduce as closely as possible the operating conditions of the compact spectrograph/detector under development for space applications, the intensifier gain was maintained at a low constant value (G=1800). The difference of slope between the calibration curves obtained with and without temporal resolution is greater at 7 Torr of CO_2 (factor of 4 difference) than at atmospheric pressure in air (factor of 1.3 difference). The fast expansion of the plasma at reduced pressure results in a rapid escape of excited species from the observation region and a greater loss of emission signal with time delay than observed at atmospheric pressure. Fig. 4 compares the Relative Standard Deviation (RSD) calculated for each element as a mean value obtained from all studied samples, at 7 Torr of CO_2 and at atmospheric pressure in air, with and without temporal resolution. In air at atmospheric pressure, the RSD is approximately the same with and without temporal resolution. At 7 Torr of CO_2, the RSD is generally lower without temporal resolution. For the major elements, the RSD is lower at 7 Torr of CO_2 than at atmospheric pressure in air. This may be related to reduced self-

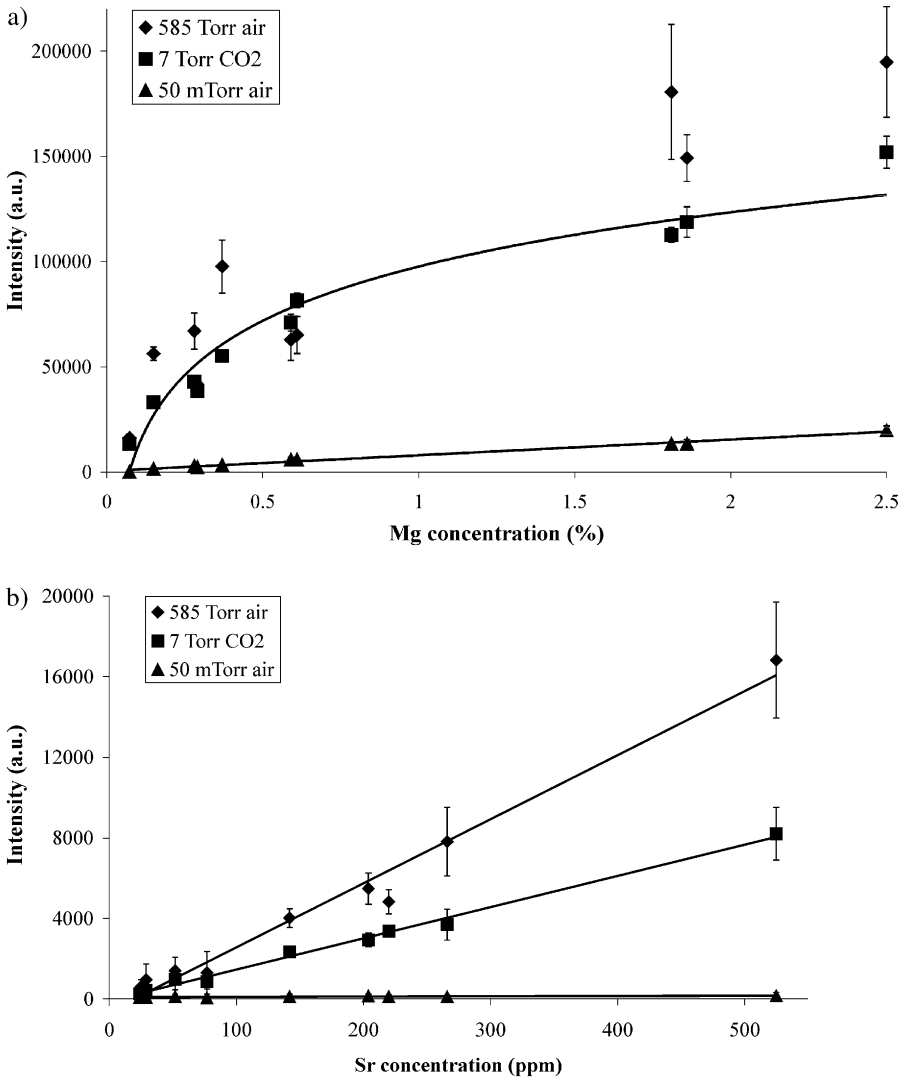

Fig. 5. Calibration curves prepared from soils at different pressures: a) for Mg (280.2 nm) and b) for Sr (407.7 nm).

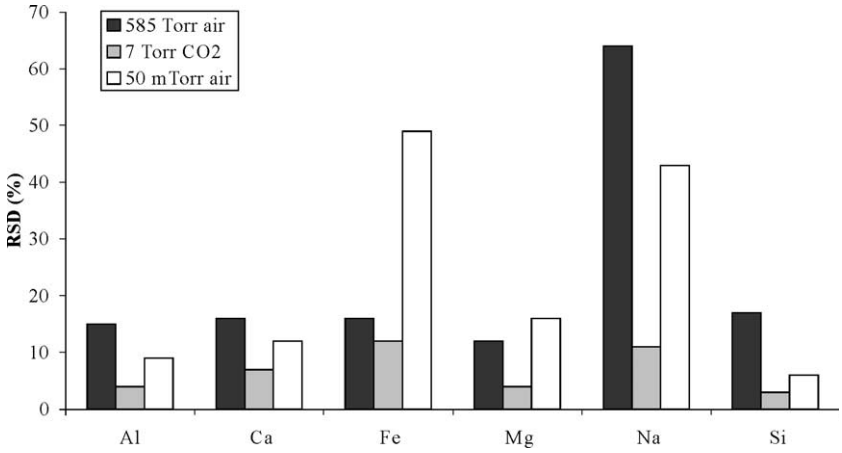

Fig. 6. Relative Standard Deviation (RSD) obtained from calibration curves in soils at three different pressures.

absorption and line broadening effects (which may be sensitive to shot-to-shot differences in plasma formation) of major species at the lower pressure. But for the minor elements (except for Sr), the RSD is lower at atmospheric pressure in air than at 7 Torr of CO_2.

At Mars pressure, using no temporal resolution seems to be a good solution for quantitative analysis because emission signals and calibration curve sensitivity are greater compared to time-resolved detection. In addition, the RSD values are lower at 7 Torr of CO_2 for no time delay. From this study, we can conclude that non-gated detectors can be used for LIBS analysis at reduced pressures for space applications. In the studies with the ESA 3000 Echelle spectrograph described below, we used no time delay and a gate width of 1 ms as acquisition parameters of plasma light.

3.3. Influence of the pressure on calibration curves

Fig. 5 shows the calibration curves obtained from soils at three different pressures for Mg (major element, line at 280.2 nm) and Sr (minor element, line at 407.7 nm) using lines of once-ionized species. Comparison of the curves shows a systematic decrease in the slope of the curve (the analytical sensitivity) with decreased pressure. At atmospheric pressure in air or at 7 Torr of CO_2, and high concentrations, the curves show a relative loss in intensity due to self-absorption of the strong 280.2 nm Mg line. At atmospheric pressure in air, it is impossible to obtain linear calibration curves for the elements Al, Ba, Ca, Cr, Fe, Mn, and Si. Whatever the chosen line, we observe pronounced scatter in the individual points of the curves. With a pressure decrease, the linear regression coefficient of the calibration curves increases. Fig. 6 demonstrates that RSD values calculated for the major elements are the lowest at 7 Torr of CO_2, that is, at Mars pressure conditions.

If we do not take into account the light collection system, the number of each species excited in the plasma formed at reduced pressure may be more important than at atmospheric pressure and may result in greater signal stability and repeatability. At lower pressures a greater number of each

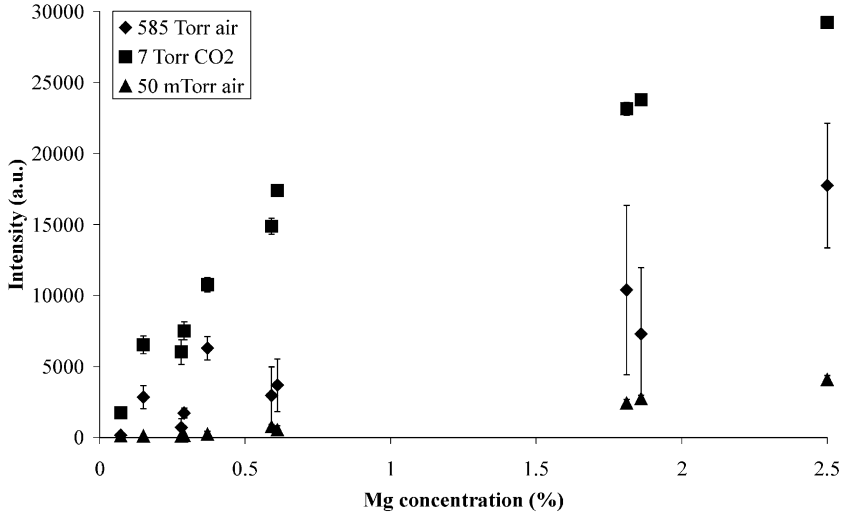

Fig. 7. Calibration curves prepared from soils at different pressures for Mg (280.2 nm) when the optical fibre is placed near the plasma (no imaging of light on fibre end).

species is ablated because of reduced plasma shielding [1]. In addition, with reduced shielding, the reproducibility of the mass ablated on each shot may be increased because shot-to-shot perturbations of the pulse energy reaching the surface to produce ablation may be less. This could explain the better RSD obtained at 7 Torr of CO_2 and also the better linear regression obtained for calibration curves with the pressure decrease. The improved correlation coefficient observed at lower pressures, that is, reduced scatter in the data, is probably due to reduced chemical matrix effects. As discussed below, at the lower pressures, the plasma will be less dense and there will be fewer interactions between species in the plasma. We can also argue that self-absorption is less important with the pressure decrease, resulting in improved calibration curves. At 50 mTorr in air, the observed increase of the RSD can be attributed to the low detected emission signal which makes difficult the calculation of background subtracted signal.

These results show that Martian pressure is favourable for quantitative analysis by the LIBS technique because we observe a better linear regression of calibration curves and lower RSD values at 7 Torr of CO_2. On the other hand, the systematic decrease in the slope of the curves with decreased pressure indicates the need for enhanced instrument capabilities at pressures of 50 mTorr and below.

3.4. Influence of plasma light collection system on calibration curves

The difference in the plasma expansion (or size of the plasma volume) with the ambient pressure has implications for the method of light collection, e.g. optical fibre directly positioned near the plasma with no imaging of light onto the fibre or imaging of the plasma light on fibre optic end with a lens (Fig. 1). We compared the results described above (obtained by imaging the plasma light on the optical fibre end) with results obtained by placing the fibre optic near the plasma with no imaging. Fig. 7 shows the calibration curves of Mg (280.2 nm) prepared from soils for the latter light collection condition and the three different pressures. The variations of intensity with the concentrations observed in this configuration are the same as those obtained by imaging the plasma light on the optical fibre (Fig. 5a). A loss of signal is observed for all the pressures when the optical fibre is placed near the plasma. This loss is more important at atmospheric pressure in air. Table 3 indicates that for all pressures studied, the RSD is higher when the optical fibre is placed near the plasma (no imaging). The RSD increase is more important at atmospheric pressure in air. These observations could be explained by the comparison of geometric extent (or etendue) of the two optical configurations. With the optical configuration of 1:1 magnification, the geometric extent is the product of the plasma image area on the optical fibre entrance which is limited by the fibre core surface area (1 mm diameter) with the solid angle of the fibre. Whatever the plasma diameter, the geometric extent is of 4.10^{-2} mm^2str and the luminous flux collected by the fibre will only depend on the plasma luminance. With the optical fibre placed near the plasma (about 15 cm), the geometric extent depends on the plasma diameter contained in the numerical aperture of the fibre. For a plasma diameter of 10 mm, it is of 3.10^{-3} mm^2str that is 14 times smaller compared to the previous configuration. The luminous flux collected by the fibre will depend on the plasma diameter and on its luminance.

As a conclusion, the loss of signal with decreasing pressure below 7 Torr has implications for the use of LIBS at low pressures (e.g., in the 50 mTorr range): it indicates that analysis at stand-off distances in such conditions will require more efficient light collection and recording methods. With the two systems of plasma light collection and for all the studied elements, we obtained calibration curves with better linear regression and the best RSD for a pressure of 7 Torr in CO_2 (Figs. 5—7 and Table 3). It could be explained as a result of lower absorption of laser energy in the plasma leading to greater ablated mass and fewer collisions between the atoms at reduced pressures inducing a more stable plasma through a decrease in matrix effects as discussed below.

3.5. Matrix effects

Fig. 8 shows a comparison of calibration curves obtained for Ca (393.3 nm) in soils and clays at different pressures. At atmospheric pressure in air and 7 Torr of CO_2 (Fig. 8a and b), the emission signals (calibration curves) obtained in the soil and clay matrices are different.

Table 3
Relative standard deviation (RSD in %) obtained from calibration curves in soils at three different pressures by imaging the plasma light on the optical fibre end and by direct plasma light collection (no imaging of light on fibre end)

Element (line)	Imaging of plasma light on the optical fibre end			No imaging of plasma light on the optical fibre end		
	585 Torr air	7 Torr CO_2	50 mTorr air	585 Torr air	7 Torr CO_2	50 mTorr air
Al (396.15 nm)	15	4	9	55	5	23
Ca (393.37 nm)	16	7	12	57	6	22
Fe (406.29 nm)	16	12	49	40	43	31
Mg (280.32 nm)	12	4	16	47	7	38
Na (588.99 nm)	64	11	43	46	35	60
Si (288.16 nm)	17	3	6	84	4	11

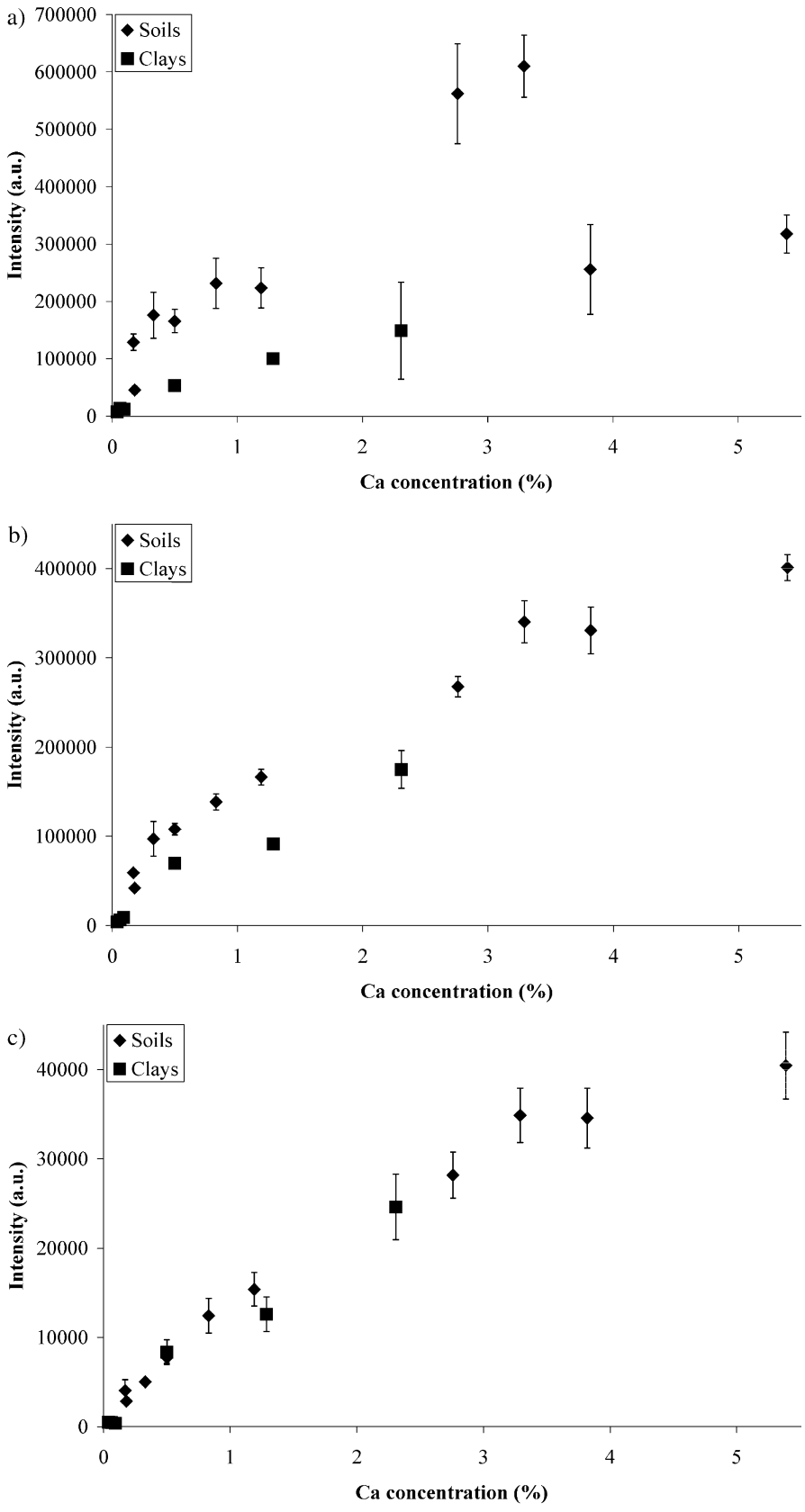

Fig. 8. Calibration curves of Ca (393.3 nm) prepared from certified soils and clays: a) at atmospheric pressure in air; b) at 7 Torr of CO_2 and c) at 50 mTorr in air.

The emission intensity for the soil matrix is greater than the intensity for the clay matrix. At atmospheric pressure, Wisbrun et al. [36] found that emissions from sand were greater than those from soil, which is consistent with Eppler et al. observation [37] of greater slopes for calibration curves obtained from the sand matrices than the slopes for the soil matrices. These latter authors showed that neither aerosol production above the sand and soil samples nor absorptivity nor particle size affected the observed differences in emissions from the sand and soil matrices. They found that the electron density of the plasma obtained from pure sand was lower than those obtained from pure soil and that the plasma temperature, however, remained constant. They suggested that elements found at appreciable concentrations in the soil matrix may have produced the increased electron density of the plasma formed on soil, since these elements all have lower ionization potentials than Si and O, the major components of the sand matrix. The greater electron density of the plasma formed on soil reduced the concentration of ions in the plasma through ion-electron recombination, decreasing the observed emission intensity from the ion lines. But this analysis could not explain the differences in the slopes of the calibration curves for the neutral species. In our measurements, the elements found at appreciable concentrations in soils and clays are similar, only the relative concentrations are different. The explanations of the previous study cannot be applied to our work here, and other mechanisms are operating that affect emission intensities.

Fig. 8 shows that the difference in emission intensities of plasmas formed on soil and clay samples decreases with the pressure decrease and becomes nonsignificant at 50 mTorr in air (Fig. 8c). The same behaviour was observed for all studied elements. This indicates that the matrix effects are pressure dependent. Chemical matrix effects can be due to interactions (collisions, electric fields) of atoms in close proximity such as in a dense plasma. As the pressure is reduced, the number of collisions between atoms in the plasma decreases so such matrix effects are reduced. Another explanation for the decrease of matrix effects at lower pressures could be different interaction regimes at different pressures inducing a difference in mass removal from the two types of sample, depending on the ambient pressure. Absorption of incident laser energy by the plasma via Inverse Bremsstrahlung (IB) increases with wavelength increase and is more effective with denser plasmas. This effect is more important at atmospheric pressure than at reduced pressure. Thus near vacuum, we could suppose a more direct interaction between the laser pulse and the sample due to reduced absorption by the plasma above the surface. With the higher laser power densities, the physical and chemical properties of the samples may have a reduced influence on the laser-matter interaction process at reduced pressure and the mass removed from soils and clays could be similar. Again, with the pressure increase, the plasma density increases inducing a more effective IB process. A greater part of laser energy is absorbed in the plasma inducing a shielding of the sample surface from the laser radiation and a decrease in the mass of vaporized matter in the plasma. The interaction could be dominated by a laser-plasma and plasma-surface interaction regime, which could be material dependent. This could explain why the laser pulse may remove more material from soils than from clays at higher pressures. But further experiments would be needed to demonstrate these effects and understand the difference of emission intensity observed between soils and clays at different pressures. These results only allow us to conclude that reduced pressures are favourable for LIBS analysis of elements found in different matrices, as the matrix effects appear less important at lower pressures.

4. Conclusion

This paper was focused on the use of the LIBS technique for analysis of geological samples on planetary surfaces. We have studied the influence of the ambient pressure (50 mTorr in air to begin to simulate the Moon or asteroids, 7 Torr of CO_2 for Mars, and atmospheric pressure in air for the Earth) on the calibration curves prepared from certified soil and clay pellets. The results show that useful calibration curves can be obtained at reduced pressure without temporal resolution of the emission signal. The best linear regression coefficient and the best repeatability are obtained at 7 Torr of CO_2 for Martian conditions. We have also shown that the method of plasma light collection had implications on the analytical results obtained at reduced pressures. We have observed a systematic decrease in the slope of the curves (the sensitivity) with decreasing pressure when the plasma light was imaged on an optical fibre end. When the plasma light was collected by a bare fibre with no imaging on the fibre end, however, the calibration curve for 7 Torr showed the greatest sensitivity. For both collection methods, the lowest signals were obtained at the lowest pressure of 50 mTorr. This indicates the need for enhanced instrument capabilities or plasma light collection at lower pressures. Finally, comparison of the calibration curves obtained in soils and clays showed that matrix effects appear less important at reduced ambient pressures. Quantitative LIBS analysis of elemental abundances regardless of the chemical matrices will be favoured in the atmospheric pressure environments of the Moon and asteroids.

Acknowledgments

B. Sallé thanks the Los Alamos National Laboratory (LANL) for the support given during this work and the

CNES, the French national institute for space research, which has permitted this exchange program.

References

[1] A.K. Knight, N.L. Scherbarth, D.A. Cremers, M.J. Ferris, Characterization of laser-induced breakdown spectroscopy (LIBS) for applications to space exploration, Appl. Spectrosc. 54 (2000) 331–340.

[2] R.C. Wiens, R.E. Arvidson, D.A. Cremers, M.J. Ferris, J.D. Blacic, F.P. Seelos IV, K.S. Deal, Combined remote mineralogical and elemental identification from rovers: field and laboratory tests using reflectance and laser-induced breakdown spectroscopy, J. Geophys. Res. 107 (2002) .

[3] R. Brennetot, J.L. Lacour, E. Vors, A. Rivoallan, D. Vailhen, S. Maurice, Mars analysis by laser-induced breakdown spectroscopy (MALIS): influence of Mars atmosphere on plasma emission. Study of factors influencing plasma emission with the use of Doehlert designs, Appl. Spectrosc. 57 (2003) 744–752.

[4] Z.A. Arp, D.A. Cremers, R.D. Harris, D.M. Oschwald, G.R. Parker Jr., D.M. Wayne, Feasibility of generating a useful laser-induced breakdown spectroscopy plasma on rocks at high pressure: preliminary study for a Venus mission, Spectrochim. Acta, Part B: Atom. Spectrosc. 59 (2004) 987–999.

[5] B. Sallé, J.L. Lacour, E. Vors, P. Fichet, S. Maurice, D.A. Cremers, R.C. Wiens, Laser-induced breakdown spectroscopy for Mars surface analysis: capabilities at stand-off distances and detection of chlorine and sulfur elements, Spectrochim. Acta, Part B: Atom. Spectrosc. 59 (2004) 1413–1422.

[6] F. Colao, R. Fantoni, V. Lazic, A. Paolini, G.G. Ori, L. Marinangeli, A. Baliva, Investigation of LIBS feasibility for in-situ planetary exploration: an analysis on Martian rock analogues, Planet. Space Sci. 52 (2004) 117–123.

[7] P. Fichet, P. Mauchien, C. Moulin, Determination of impurities in uranium and plutonium dioxides by laser induced breakdown spectroscopy, Appl. Spectrosc. 53 (1999) 1111–1117.

[8] P. Fichet, P. Mauchien, J.F. Wagner, C. Moulin, Quantitative elemental determination in water and oil by laser induced breakdown spectroscopy, Anal. Chim. Acta 429 (2001) 269–278.

[9] M. Tran, Q. Sun, B. Smith, J.D. Winefordner, Direct determination of trace elements in terephthalic acid by laser induced breakdown spectroscopy, Anal. Chim. Acta 419 (2000) 153–158.

[10] M. Hanafi, M.M. Omar, Y.E.E.D. Gamal, Study of laser-induced breakdown spectroscopy of gases, Radiat. Phys. Chem. 57 (2000) 11–20.

[11] J. Bublitz, C. Dölle, W. Schade, A. Hartmann, R. Horn, Laser induced breakdown spectroscopy for soil diagnostics, Eur. J. Soil Sci. 52 (2001) 305–312.

[12] M.C. Boiron, J. Dubessy, N. André, A. Briand, J.L. Lacour, P. Mauchien, J.M. Mermet, Analysis of mono-atomic ions in individual fluid inclusions by laser-produced plasma emission spectroscopy, Geochim. Cosmochim. Acta 55 (1991) 917–923.

[13] D. Ohnenstetter, W.L. Brown, Compositional variation and primary water contents of differentiated interstitial and included glasses in boninites, Contrib. Mineral. Petrol. 123 (1996) 117–137.

[14] C. Fabre, M.C. Boiron, J. Dubessy, A. Moissette, Determination of ions in individual fluids by laser ablation optical emission spectroscopy, J. Anal. At. Spectrom. 14 (1999) 913–922.

[15] B.C. Clark, A.K. Baird, H.J. Rose Jr., P. Toulmin, R.P. Christian, W.C. Kelliher, A.J. Castro, C.D. Rowe, K. Keil, G.R. Huss, The Viking X ray fluorescence experiment: analytical methods and early results, J. Geophys. Res. 82 (1977) 4577–4594.

[16] J. Bruckner, G. Dreibus, R. Rieder, H. Wanke, Lunar and Planetary Science, XXXII, Lunar and Planetary Institute, Houston, TX, 2001. abstr. 1293.

[17] R. Rieder, T. Economou, H. Wanke, A. Turkevich, J. Crisp, J. Bruckner, D. Dreibus, H.Y. McSween Jr., The chemical composition of Martian soil and rocks returned by the mobile alpha proton X-ray spectrometer: preliminary results from the X-ray mode, Science 278 (1997) 1771–1774.

[18] D.A. Cremers, The analysis of metals at a distance using laser-induced breakdown spectroscopy, Appl. Spectrosc. 41 (1987) 572–578.

[19] S. Palanco, J.M. Baena, J.J. Laserna, Open-path laser-induced plasma spectrometry for remote analytical measurements on solid surfaces, Spectrochim. Acta, Part B: Atom. Spectrosc. 57 (2002) 591–599.

[20] K. Kagawa, M. Ohtani, S. Yokoi, S. Nakajima, Characteristics of the plasma induced by the bombardment of N_2 laser pulse at low pressures, Spectrochim. Acta, Part B: Atom. Spectrosc. 39 (1984) 525–536.

[21] Y. Iida, Effects of atmosphere on laser vaporization and excitation processes of solid samples, Spectrochim. Acta, Part B: Atom. Spectrosc. 45 (1990) 1353–1367.

[22] Y.I. Lee, T.L. Thiem, G.H. Kim, Y.Y. Teng, J. Sneddon, Interaction of an excimer-laser beam with metals. Part III: the effect of a controlled atmosphere in laser-ablated plasma emission, Appl. Spectrosc. 46 (1992) 1597–1604.

[23] M. Kuzuya, O. Mikami, Effect of argon pressure on spectral emission of a plasma produced by a laser microprobe, J. Anal. At. Spectrom. 7 (1992) 493–497.

[24] D.B. Geohegan, A.A. Puretzky, Dynamics of laser ablation plume penetration through low pressure background gases, Appl. Phys. Lett. 67 (1995) 197–199.

[25] H. Kurniawan, W.S. Budi, M.M. Suliyanti, A.M. Marpaung, K. Gagawa, Characteristics of a laser plasma induced by irradiation of a normal-oscillation YAG laser at low pressures, J. Phys., D. Appl. Phys. 30 (1997) 3335–3345.

[26] Y.I. Lee, K. Song, H.K. Cha, J.M. Lee, M.C. Park, G.H. Lee, J. Sneddon, Influence of atmosphere and irradiation wavelength on copper plasma emission induced by excimer and Q-switched Nd:YAG laser ablation, Appl. Spectrosc. 51 (1997) 959–964.

[27] B.Y. Man, X.T. Wang, G.T. Wang, Effect of ambient pressure on the generation and the propagation of plasmas produced by pulsed laser ablation of metal Al in air, Appl. Spectrosc. 51 (1997) 1910–1915.

[28] J.M. Vadillo, J.M. Fernandez Romero, C. Rodriguez, J.J. Laserna, Effect of plasma shielding on laser ablation rate of pure metals at reduced pressure, Surf. Interface Anal. 27 (1999) 1009–1015.

[29] M. Noda, Y. Deguchi, S. Iwasaki, N. Yoshikawa, Detection of carbon content in a high-temperature and high-pressure environment using laser-induced breakdown spectroscopy, Spectrochim. Acta, Part B: Atom. Spectrosc. 57 (2002) 701–709.

[30] S.I. Gornushkin, I.B. Gornushkin, J.M. Anzano, B.W. Smith, J.D. Winefordner, Effective normalization technique for correction of matrix effects in laser-induced breakdown spectroscopy detection of magnesium in powdered samples, Appl. Spectrosc. 56 (2002) 433–436.

[31] B. Sallé, D.A. Cremers, K. Benelli, J. Busse, R.C. Wiens, S. Maurice, R. Walters, Evaluation of a compact spectrograph/detection system for a LIBS instrument for in-situ and stand-off detection, Lunar and Planetary Science, XXXV, Lunar and Planetary Institute, Houston, TX, 2004. abstr. 1263.

[32] P.R. Christensen, H.J. Moore, in: H.H. Kieffer, B.M. Jakosky, C.W. Snyder, M.S. Matthews (Eds.), The Martian Surface Layer, in Mars, University of Arizona Press, Tucson, AZ, 1992.

[33] M.K. Mazumder, D. Saini, A.S. Biris, P.K. Srirama, C. Calle, C. Buhler, Mars dust: characterization of particle size and electrostatic charge distributions, Lunar and Planetary Science, XXXV, Lunar and Planetary Institute, Houston, TX, 2004. abstr. 2022.

[34] N. André, C. Geertsen, J.L. Lacour, P. Mauchien, S. Sjostrom, UV laser ablation optical emission spectrometry on aluminum alloys in air

at atmospheric pressure, Spectrochim. Acta, Part B: Atom. Spectrosc. 49 (1994) 1363–1372.
[35] M. Milan, J.M. Vadillo, J.L. Laserna, Removal of air interference in laser-induced breakdown spectrometry monitored by spatially and temporally resolved charge-coupled device measurements, J. Anal. At. Spectrom. 12 (1997) 441–444.
[36] R. Wisbrun, I. Schechter, R. Niessner, H. Schröder, K. Kompa, Detector for trace elemental analysis of solid environmental samples by laser plasma spectroscopy, Anal. Chem. 66 (1994) 2964–2975.
[37] A.S. Eppler, D.A. Cremers, D.D. Hickmott, M.J. Ferris, A.C. Koskelo, Matrix effects in the detection of Pb and Ba in soils using laser-induced breakdown spectroscopy, Appl. Spectrosc. 50 (1996) 1175–1181.